

## Renormalization-group study of the ferromagnetic Ising model on the triangular lattice

Chris Unger

*Center for Polymer Studies and Department of Physics, Boston University, Boston, Massachusetts 02215 and Texas Instruments Central Research Laboratories, P.O. Box 225936, MS 147 Dallas, Texas 75265\**

(Received 21 November 1983; revised manuscript received 12 March 1984)

The dynamic real-space renormalization group of Mazenko and Valls is applied to the zero-field ferromagnetic Ising model on the triangular lattice. Renormalization equations valid for all temperatures above the critical temperature  $T_c$  are derived for the susceptibility, specific heat, structure factor, and correlation length. The magnetization is found for  $T < T_c$ . The critical exponents and amplitudes for these quantities are calculated. The agreement between the known static properties and the renormalization-group results is good to excellent, and shows that this renormalization-group method can accurately calculate nonuniversal, as well as universal, quantities on different lattices. The computed dynamic structure factor, however, exhibits nonmonotonic behavior as a function of temperature. This nonmonotonic behavior is conjectured to be due to approximations in determining the expansion parameters.

### I. INTRODUCTION

The renormalization-group method is acknowledged to be one of the most intuitively appealing and useful ways of treating systems at their critical point.<sup>1</sup> Largely ignored but implicit in the real-space renormalization group is its ability to treat the entire phase diagram, not just the critical point.<sup>1,2</sup> Although there have been calculations of static properties away from the critical point,<sup>2</sup> most dynamic renormalization-group treatments obtain only the critical-point time-rescaling exponent  $z$ .<sup>3</sup>

There are two difficulties that must be handled before the renormalization group can treat general length and time scales. Both the long- and short-range correlations must be included in the treatment if the nonsingular behavior is to be obtained, and long-range couplings in the renormalized Hamiltonian must be treated or eliminated. Most formalisms treat only the longest-length scales correctly and hence derive only the singular behavior at critical points, where the length scales are infinite. Mazenko *et al.*<sup>4,5</sup> include short-range information by introducing a projection operator to separate the long- from the short-length scales and treat the short-wavelength fluctuations by perturbation theory; the critical fluctuations are treated as usual by renormalization.

The long-range spatial correlations in the renormalized Hamiltonian can be treated by truncation<sup>1</sup> or Monte Carlo methods.<sup>6</sup> The long-time correlations lead to a non-Markovian renormalized spin-flip operator. These nonlocal temporal correlations are more difficult to eliminate than the nonlocal spatial correlations. They must be eliminated, however, since it is not clear whether a non-Markovian spin-flip operator is in the same universality class as the original one. In order to eliminate the non-Markovian effects in the renormalized spin-flip operator and preserve its form, Mazenko *et al.*<sup>4,5</sup> introduce an eigenvalue equation that the renormalization transformation must satisfy.

Mazenko and Valls find reasonable values for the equilibrium dynamic structure factor for the two-

dimensional Ising model on the square lattice, both above<sup>5</sup> and below<sup>7</sup> the critical temperature  $T_c$ . They also obtain a good agreement with experimental results for the nonequilibrium evolution of the time-dependent structure factor for quenched systems.<sup>8</sup> These good results are obtained from a first-order expansion in the coupling between cells. In contrast, the low-order cumulant expansions<sup>1</sup> predict qualitatively the wrong decay of correlations when used away from the critical point.<sup>5</sup>

In this paper, I extend the method of Mazenko and Valls to the triangular lattice in order to determine whether their method can accurately determine both universal and nonuniversal quantities on different lattices. If the method can accurately obtain lattice-dependent quantities, then it can also be used to study models with frustration. These models often have a glass transition where the length and time scales are not infinite, and hence standard renormalization-group methods are not appropriate. Frustration is a lattice-dependent quantity; the nearest-neighbor Ising model on the square lattice cannot be frustrated, while the antiferromagnetic nearest-neighbor coupling on the triangular lattice leads to frustrated triangular plaquettes.

The calculated results for the static properties of the Ising model on the triangular lattice compare favorably with known values of both the universal and lattice-dependent quantities for all temperatures and wavelengths studied. These good results are obtained from a lowest-order expansion with the effective parameters determined with the use of known short-range correlations. The results of an analogous calculation for the dynamics, although generally reasonable, have qualitatively incorrect features not found in the results of a similar calculation on the square lattice. I conjecture that the dynamical recursion relations are more sensitive than the static equations. The small errors I make in approximating the time-rescaling parameter (which can be evaluated exactly on the square lattice) may be the cause of the nonmonotonic behavior of the dynamic structure factor which I obtain.

This paper is organized as follows. In Sec. II, I introduce an expansion in a small intercell coupling parameter, introduce the renormalization transformation, define the projection operator which separates long-wavelength from short-wavelength fluctuations, and obtain the temperature recursion relation. I use the projection operator to derive formal recursion relations for static quantities in Sec. III. The static quantities treated are two- or four-spin-correlation functions, but the method can be applied to functions of any number of spins. From the recursion relation for the correlation between any two spins, I calculate the recursion relation for the susceptibility and the correlation length. The recursion relations for the magnetization, a single-spin correlation, and the specific heat, a four-spin correlation, are also found. In Sec. IV I specify the parameters appearing in the formal relations, and obtain numerical results. The results for general temperature (and various wavelengths for space-dependent averages) are plotted; in addition, the recursion relations are analyzed to obtain critical exponents and amplitudes. I compare the numerical answers with previous results for the static quantities as a function of temperature and wavelength. In Sec. V the formalism for the dynamical correlation functions is presented. I derive the recursion relations and present the numerical results for space- and time-dependent spin-correlation functions and the dynamic structure factor, and discuss the numerical difficulties in Sec. VI. The results are summarized in Sec. VII.

## II. FORMALISM

I consider the Ising model on a triangular lattice with Hamiltonian

$$H(\sigma) = K \sum_{\langle ij \rangle} \sigma_i \sigma_j,$$

where a factor of  $-\beta$  has been absorbed in the definition of the coupling constant  $K$  and  $\langle ij \rangle$  indicates that  $i$  and  $j$  are neighboring sites. I divide the lattice into cells, each containing three spins, and introduce vectors  $\vec{i}$  to label the cell, and vectors  $\vec{\delta}_a$ ,  $a=1,2,3$  to label the position of the spin within the cell (see Fig. 1). The notation  $\sigma_{i,a}$  is introduced for the spin at the lattice site  $\vec{i} + \vec{\delta}_a$ .

In order to treat the coupling between cells as a small

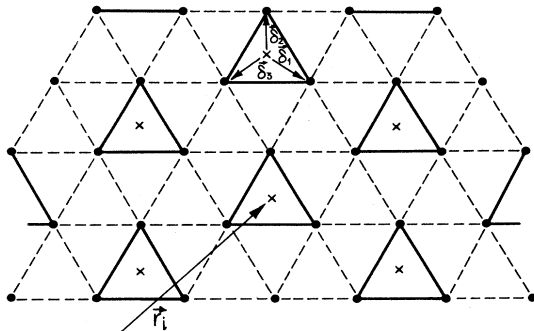


FIG. 1. Diagram of the triangular lattice showing the bonds inside a cell as solid lines and bonds between cells as dotted lines. Crosses indicate where the renormalized spins are situated after a renormalization operation.

parameter, the Hamiltonian is separated into intracell  $H_0$  and intercell  $H_I$  contributions:

$$H(\sigma) = H_0(\sigma) + H_I(\sigma) = K_C V_0(\sigma) + K_I V_I(\sigma), \quad (2.1a)$$

where

$$V_0(\sigma) = \sum_{i,a} \sigma_{i,a} \sigma_{i,a+1} \quad (2.1b)$$

and

$$V_I(\sigma) = \sum_{i,a} \sigma_{i,a} (\sigma_{i+3\vec{\delta}_a, a+1} + \sigma_{i+3\vec{\delta}_a, a-1} + \sigma_{i+3\vec{\delta}_{a-1}, a-1} + \sigma_{i+3\vec{\delta}_{a+1}, a+1}). \quad (2.1c)$$

The solid lines in Fig. 1 represent the bonds in the intracell coupling  $V_0$ ; the dotted lines represent the bonds comprising the intercell coupling  $V_I$ . I introduce a parameter  $\lambda$  and rewrite the Hamiltonian as

$$H(\sigma) = \{K_C(\lambda) + \lambda[K - K_C(\lambda)]\} V_0(\sigma) + \lambda\{K_I(\lambda) + \lambda[K - K_I(\lambda)]\} V_I(\sigma). \quad (2.2)$$

The parameter  $\lambda$  measures the strength of the intercellular coupling;  $\lambda=1$  corresponds to isotropic couplings  $K_C = K_I = K$ , while at  $\lambda=0$ ,  $V_I$  does not appear in  $H$ . If I were to expand  $K_C$  and  $K_I$  in Eq. (2.1a) directly in powers of  $\lambda$ , the isotropy condition at  $\lambda=1$  would be difficult to satisfy order by order; in contrast, the Hamiltonian in Eq. (2.2) automatically becomes isotropic as  $\lambda \rightarrow 1$ . I expand  $K_C(\lambda)$  and  $K_I(\lambda)$  order by order:

$$K_C(\lambda) = \sum_n K_n^C \lambda^n, \quad (2.3a)$$

$$K_I(\lambda) = \sum_n K_n^I \lambda^n, \quad (2.3b)$$

and obtain the Hamiltonian to first order in  $\lambda$ :

$$H(\sigma) = K_0^C V_0(\sigma) + \lambda[\Delta K_1 V_0(\sigma) + K_0^I V_I(\sigma)] \quad (2.4)$$

with  $\Delta K_1 = K - K_0^C + K_1^C$ . The partition function to first order in  $\lambda$  can be written as

$$Z = \sum_{\sigma} e^{H(\sigma)} = Z_0 [1 + \lambda \Delta K_1 N r + O(\lambda^2)], \quad (2.5)$$

where  $N$  is the total number of spins,  $Z_0$  is the partition function for uncoupled cells,  $r$  is the intracell nearest-neighbor correlation function

$$r = \langle \sigma_{i,a} \sigma_{i,a \pm 1} \rangle_0 = \frac{a_0}{2 - a_0}, \quad (2.6)$$

and

$$a_0 = \tanh(2K_0^C). \quad (2.7)$$

The equilibrium probability distribution  $P(\sigma)$  is

$$P(\sigma) = \frac{e^{H(\sigma)}}{Z} = P_0(\sigma) [1 + \lambda \delta H_1(\sigma) + O(\lambda^2)] \quad (2.8a)$$

with

$$P_0(\sigma) = \frac{e^{K_0 V_0(\sigma)}}{Z_0} \quad (2.8b)$$

and

$$\delta H_1 = \Delta K_1 [V_0(\sigma) - \langle V_0(\sigma) \rangle_0] + K_0^I V_I(\sigma). \quad (2.8c)$$

The renormalization group is implemented by a coarse-graining transformation  $T(\mu, \sigma)$ , which maps operators on the original lattice onto coarse-grained or renormalized operators on the new lattice by the relations

$$P(\mu) = \sum_{\sigma} P(\sigma) T(\mu, \sigma) \quad (2.9)$$

and

$$A(\mu) P(\mu) = \sum_{\sigma} A(\sigma) P(\sigma) T(\mu, \sigma). \quad (2.10)$$

In order to preserve the normalization of the probability distribution on the new lattice,

$$\sum_{\mu} T(\mu, \sigma) = 1 \quad (2.11)$$

must be satisfied. I follow Mazenko and Valls<sup>5</sup> and introduce the additional requirement

$$\langle T(\mu, \sigma) T(\mu', \sigma) \rangle = \delta_{\mu, \mu'} P(\mu), \quad (2.12)$$

where

$$\delta_{\mu, \mu'} = \prod_{j=1}^{N'} \delta_{\mu_j \mu'_j}.$$

This condition implies that a single-spin operator on the original lattice is mapped onto a single-spin operator on the renormalized lattice. The operator  $P$ , defined by

$$PA(\sigma) = \sum_{\sigma'} \sum_{\mu} \frac{T(\mu, \sigma) T(\mu, \sigma')}{P(\mu)} A(\sigma') P(\sigma'), \quad (2.13)$$

is a projection operator, namely,  $P^2 = P$ ; this identity is derived with the use of Eq. (2.12). When applied to a function  $A(\sigma)$ ,  $P$  selects those parts which are mapped onto the coarse-grained function  $A(\mu)$ :

$$\begin{aligned} \sum_{\sigma} T(\mu, \sigma) [PA(\sigma)] P(\sigma) &= A(\mu) P(\mu) \\ &= \sum_{\sigma} T(\mu, \sigma) A(\sigma) P(\sigma). \end{aligned} \quad (2.14)$$

Thus,  $QA(\sigma) \equiv (1-P)A(\sigma)$  is the short-range part of  $A(\sigma)$ , which renormalizes to 0. These short-range fluctuations can be treated by perturbative techniques. I note the further useful identities involving  $P$ :

$$\langle PA(\sigma) \rangle = \langle A(\mu) \rangle \quad (2.15a)$$

and

$$\langle PA(\sigma) PB(\sigma) \rangle = \langle A(\mu) B(\mu) \rangle. \quad (2.15b)$$

To obtain an explicit form for  $T(\mu, \sigma)$  to zeroth order in  $\lambda$ , I write  $T$  in the independent-cell approximation as follows:

$$T(\mu, \sigma) = \prod_{i=1}^{N'} T^{(i)}(\mu_i, \sigma_{i,a}). \quad (2.16)$$

In the absence of a magnetic field, the most general form

of  $T^{(i)}$  which satisfies the constraints (2.11) and (2.12) can be written as

$$T^{(i)}(\mu_i, \sigma_{i,a}) = \frac{1}{2} [1 + \mu_i \psi(\sigma_{i,a})], \quad (2.17)$$

where

$$\langle \psi(\sigma_{i,a}) \rangle_0 = 0, \quad (2.18a)$$

$$\langle \psi^2(\sigma_{i,a}) \rangle_0 = 1. \quad (2.18b)$$

In order that the coarse-grained variable corresponding to a single spin is also a single spin, I take  $\psi$  to be a weighted sum of single-spin variables. Isotropy considerations imply<sup>9</sup> that each spin in the cell must be weighted equally:

$$\psi(\sigma_{i,a}) = n_1 \sum_a \sigma_{i,a}, \quad (2.19a)$$

where

$$n_1 = \frac{1}{\left\langle \left[ \sum_a \sigma_{i,a} \right]^2 \right\rangle_0} = \frac{1}{[3(1+2r)]^{1/2}}. \quad (2.19b)$$

I show in Sec. VI that this choice of  $\psi$  is also appropriate for the dynamics.

I use the method developed previously<sup>4,5</sup> to find the first-order contributions to  $P(\sigma)$  and  $T(\mu, \sigma)$ . By breaking up the calculation of  $T$  into first finding its "magnitude" and then finding its "direction," the algebra involved is greatly reduced. I construct

$$\bar{T}(\mu, \sigma) = T_0(\mu, \sigma) + \lambda \bar{T}_1(\mu, \sigma) + O(\lambda^2)$$

with the constraint that

$$\langle T_0(\mu, \sigma) \bar{T}_1(\mu', \sigma) \rangle_0 = 0.$$

Then I construct a rotation which diagonalizes

$$G(\mu, \mu') \equiv \langle \bar{T}(\mu, \sigma) \bar{T}(\mu', \sigma) \rangle. \quad (2.20)$$

I find that  $T_1$  makes no contribution to  $\bar{G}$  to first order and that the only contribution comes from the first-order probability distribution:

$$\bar{G}(\mu, \mu') = \delta_{\mu, \mu'} \bar{P}(\mu) + \lambda \bar{\Delta}(\mu, \mu') + O(\lambda^2) \quad (2.21a)$$

with

$$\bar{P}(\mu) = P_0(\mu) [1 + 2\lambda v_1^2 K_0^I H_1(\mu) + O(\lambda^2)], \quad (2.21b)$$

$$P_0(\mu) = \left(\frac{1}{2}\right)^{N'}, \quad (2.21c)$$

$$H_1(\mu) = \sum_{\langle i,j \rangle} \mu_i \mu_j, \quad (2.21d)$$

and

$$v_1 = \langle \sigma_{i,a} \psi(\sigma_{i,a}) \rangle_0 = \left[ \frac{1+2r}{3} \right]^{1/2}. \quad (2.21e)$$

The coupling characterizing the renormalized probability distribution is

$$K' = 2v_1^2 K_0^I. \quad (2.22)$$

### III. STATIC RECURSION RELATIONS

I develop recursion relations for the pair correlation function

$$C_{ia,jb} = \langle \sigma_{i,a} \sigma_{j,b} \rangle \quad (3.1)$$

and its Fourier transform, the static structure factor,

$$\begin{aligned} \Pi_{ia,jb} &= \nu_1^2 \mu_i \mu_j (1 - \delta_{i,j}) + \delta_{i,j} [\delta_{a,b} + r(\delta_{a,b+1} + \delta_{a,b-1})] + O(\lambda) \\ &= \nu_1^2 \mu_1 \mu_j + \delta_{i,j} [\delta_{a,b} + r(\delta_{a,b+1} + \delta_{a,b-1}) - \nu_1^2] + O(\lambda). \end{aligned} \quad (3.3)$$

For completeness, I also note that the coarse-grained operator  $M_{i,a}(\mu)$  corresponding to  $\sigma_{i,a}$  is

$$M_{i,a}(\mu) = \nu_1 \mu_i + O(\lambda). \quad (3.4)$$

With the use of projection operators, Eq. (3.1) becomes

$$\begin{aligned} C_{ia,jb} = \langle \sigma_{i,a} \sigma_{j,b} \rangle &= \langle P(\sigma_{i,a} \sigma_{j,b}) \rangle + \langle Q(\sigma_{i,a} \sigma_{j,b}) \rangle \\ &= \langle \Pi_{ia,jb}(\lambda) \rangle = \nu_1^2 \tilde{C}'_{i,j} + \delta_{i,j} [\delta_{a,b} + r(\delta_{a,b+1} + \delta_{a,b-1}) - \nu_1^2], \end{aligned} \quad (3.5)$$

where a prime indicates that the quantity is defined on the course-grained lattice. I derive a recursion relation for  $\tilde{C}(q)$  by Fourier transforming Eq. (3.5), and rescaling  $N$  and  $R$ :

$$\tilde{C}(q) = \nu_1^2 f(q) \tilde{C}'(q') + \{1 + r[f(q) - 1] - \nu_1^2 f(q)\}, \quad (3.6)$$

where

$$f(q) = 1 + \frac{2}{3} \cos(q_x) + \frac{4}{3} \cos(q_x/2) \cos[(\sqrt{3}/2)q_y] \quad (3.7)$$

is the cell structure factor, and

$$q'_x = (\sqrt{3}/2)q_x + \frac{1}{2}q_y, \quad (3.8a)$$

$$q'_y = -\frac{1}{2}q_x + (\sqrt{3}/2)q_y. \quad (3.8b)$$

Note that after one renormalization, the  $x$  axis is rotated by  $30^\circ$  (or equivalently  $30^\circ \pm n60^\circ$ ) as illustrated in Fig. 2. Thus, any vector on the new lattice is related to a vector on the original lattice by a rotation as well as a rescaling.

The susceptibility  $\chi$  is related to the average over all of the spins of  $C_{ia,jb}$ , or equivalently  $C(q=0)$ . The  $q \rightarrow 0$  limit of Eq. (3.6) yields the recursion relation

$$\chi = 3\nu_1^2 \chi'. \quad (3.9)$$

The correlation length  $\xi$  can be found from the second

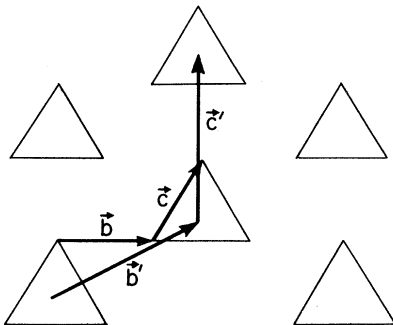


FIG. 2. Sketch of the two nearest-neighbor vectors  $\vec{b}$  and  $\vec{c}$  on both the site lattice and the renormalized cell lattice.

$$\tilde{C}(q) = \frac{1}{N} \sum_{i,a;j,b} C_{ia,jb} e^{i\vec{q} \cdot (\vec{R}_{i,a} - \vec{R}_{j,b})}. \quad (3.2)$$

In order to evaluate the long- and short-range parts of  $C_{ia,jb}$ , I require Eqs. (2.15) and the coarse-grained operator  $\Pi_{ia,jb}(\mu)$  corresponding to  $\sigma_{i,a} \sigma_{j,b}$ . For  $T > T_c$  and hence  $\langle \sigma_{i,a} \rangle = 0$ , the relation is

moment  $\mu_2$  of the static correlation function

$$\xi^2 = \frac{\mu_2}{6\chi}, \quad (3.10a)$$

where

$$\mu_2 = \frac{d^2}{N} \sum_{i,a;j,b} C_{ia,jb} (\vec{R}_{i,a} - \vec{R}_{j,b})^2, \quad (3.10b)$$

and  $d$  is the nearest-neighbor distance. In order to calculate  $\xi$ , I require a recursion relation for  $\mu_2$ . Such a recursion relation follows from Eqs. (3.5) and (3.10b) and a rescaling of  $d$  and  $N$ . The result is

$$\mu_2 = 9\nu_1^2 \mu'_2 + 2\nu_1^2 \chi' + 2(r - \nu_1^2). \quad (3.11)$$

In the following, I require the short-range correlation functions

$$\epsilon(m,n) = \frac{1}{N} \sum_{\vec{r}} \langle \sigma_{\vec{r}} \sigma_{\vec{r} + m\vec{b} + n\vec{c}} \rangle, \quad (3.12)$$

where  $\vec{b}$  and  $\vec{c}$  are linearly independent nearest-neighbor vectors, as shown in Fig. 2. Recursion relations for the short-range correlation functions of interest are

$$\epsilon(1,0) = \frac{1}{3}r + \frac{2}{3}\nu_1^2 \epsilon'(1,0), \quad (3.13a)$$

$$\epsilon(3n,0) = \nu_1^2 \epsilon'(n,n), \quad (3.13b)$$

and

$$\epsilon(n,n) = \nu_1^2 \epsilon'(n,0). \quad (3.13c)$$

I derive a recursion relation for the specific heat, defined by

$$C_H = \sum_{(ij),(kl)} (\langle \sigma_i \sigma_j \sigma_k \sigma_l \rangle - \langle \sigma_i \sigma_j \rangle \langle \sigma_k \sigma_l \rangle). \quad (3.14)$$

Each spin is temporarily labeled with one subscript for simplicity. By substituting Eq. (3.3) into Eq. (3.14), the recursion relation for  $C_H$  is found to be

$$\begin{aligned}
C_H = & \frac{4}{3}v_1^2(C'_H - 3) + 3 + 4r - 3v_1^2 \\
& + (24 - 4r - 20v_1^2)v_1^2\epsilon'(1,0) \\
& + (2 + 10r - 12v_1^2)v_1^2\epsilon'(1,1) \\
& + 4(r - v_1^2)v_1^2\epsilon'(2,0). \quad (3.15)
\end{aligned}$$

#### IV. DETERMINATION OF THE STATIC PARAMETERS AND NUMERICAL RESULTS

In order to obtain numerical results from the recursion relations derived in Sec. III, I specify the lowest-order expansions of  $K_C$  and  $K_I$ . These parameters are determined by ensuring that the pair correlation functions have the correct short- and long-range behavior. As shown in Ref. 5, most simple cumulant expansions do not predict exponential decay of spatial correlations for  $T \neq T_c$ . In order to guarantee exponential decay, I require that

$$K' \sim \begin{cases} bK, & K \gg 1 \\ K^b, & K \ll 1, \end{cases} \quad (4.1a)$$

$$(4.1b)$$

where  $b$  is the length rescaling factor, equal to  $\sqrt{3}$  with the present choice of cell.

On the square lattice,  $K'(K)$  was determined by considering the two-spin-correlation functions for spins in different cells.<sup>5</sup> This procedure cannot be used to derive a nonanalytic recursion relation, such as  $K' \sim K^{\nu}$ , which is appropriate for the triangular lattice. I note, however, that the rescaling factor  $b$  for two consecutive renormalizations is 3 and hence  $K''$  is an analytic function of  $K$ . From Eqs. (3.13b) and (3.13c) I find

$$\epsilon(3n,0) = v_1^2 v_1'^2 \epsilon''(n,0),$$

which implies

$$\frac{\epsilon(6n,0)}{\epsilon(3n,0)} = \frac{\epsilon''(2n,0)}{\epsilon''(n,0)}. \quad (4.2)$$

Series expansions of  $\epsilon(n,0)$  show that the exact solution  $K''(K)$  to Eq. (4.2) satisfies Eq. (4.1). The fixed point of Eq. (4.2) should locate the critical point; the exact correlation functions satisfy Eq. (4.2) at  $K = K'' = K_c$  to within 0.2%. Thus, I take the solution to Eq. (4.2) for  $K''(K)$  to be a check on any recursion relation for  $K'(K)$ .

In order to derive the nonanalytic recursion relation for  $K'$ , I define a function  $\varphi(K)$  and assume a recursion relation of the form  $\varphi(K') = [\varphi(K)]^b$ . The function

$$\varphi(K) = e^{4K} \frac{e^{4K} - 1}{e^{4K} + 3} \quad (4.3)$$

is a reasonable guess based on duality considerations. The recursion relation obtained with the use of this  $\varphi$  satisfies Eq. (4.1) and agrees well with Eq. (4.2). Hence, I use this form of  $\varphi$  to determine  $K'(K)$ , which is equivalent to specifying the lowest-order intercellular coupling  $K_0^I$  [see Eq. (2.22)].

Once I make a choice of  $K'(K)$ , I can determine the effective intracellular coupling  $K_0^C$ . The spins on the original lattice each "feel" six bonds of strength  $K$ , while the same spins feel two bonds of strength  $K_0^C$  to lowest order.

If I take  $K_0^C = K$ , I replace bonds of total strength  $6K$  by bonds of strength  $2K$ . If instead I take the relation  $K_0(K) \approx 3K$ , then I do not change the total strength of the bonds "felt" by any single spin. These considerations are consistent with the ideas of Migdal-Kadanoff bond moving.<sup>10</sup> I can ensure the correct magnitude for  $K_0$  by requiring that Eq. (3.13a) be satisfied by the exact nearest-neighbor correlations. Upon solving Eq. (3.13a) for  $K_0$ , I find

$$\tanh(2K_0) = \frac{2[9\epsilon(0,1) - 2\epsilon'(0,1)]}{3 + 9\epsilon(0,1) + 2\epsilon'(0,1)}. \quad (4.4)$$

With the exact solution for  $\epsilon(0,1)$ ,<sup>11</sup> Eq. (4.4) specifies the function  $K_0(K)$ . I plot  $K_0 - 3K$  versus  $\tanh K$  in Fig. 3 and observe that this quantity remains small for all  $K$ .

With  $K'(K)$  and the lowest-order expansions of  $K_C$  and  $K_I$  determined, I evaluate numerically the static correlation functions from their renormalization equations. The recursion relation for any particular pair correlation function can be solved exactly at  $T = T_c$ . Using the fact that the nearest-neighbor correlation  $\epsilon(1,0)|_{T_c} = \frac{2}{3}$ , I find the effective intercellular coupling  $\tanh(2K_0)|_{T_c} = \frac{28}{31}$ . With the use of this result I can find all pair correlation functions at the critical point. The numerical values of three short-range correlations are listed in Table I. It is seen that this method predicts their value to within 2%. Stephenson<sup>11</sup> has found the limiting long-range behavior of the correlations at the critical point:  $\epsilon(0,r) \sim A_0 r^{-\nu}$ , with  $A_0 = 0.66865$ , and  $\nu = \frac{1}{4}$ . Our calculation predicts

$$\epsilon(0,2^k) = \epsilon(0,1)(v_{1,c})^k \quad (4.5)$$

with  $A_0 = \frac{2}{3}$  and  $\nu = \ln \frac{17}{15} / \ln \sqrt{3} = 0.228$ , an error of approximately 9%. I have also compared the exact results to the renormalization-group predictions above  $T_c$ ; the accuracy is similar to that at  $T_c$ .

The second type of critical behavior associated with two-spin correlations is the divergence of the pair correlation length defined in Eq. (3.10). Iterating Eqs. (3.9) and (3.11) I find  $\xi \sim \xi_0 |(u - u_c)/u_c|^{-\nu}$  with  $\xi_0 = 0.425$ . Our choice of the recursion relation for  $K'$  implies that the exponent  $\nu$  is given exactly by the relation

$$\nu = \frac{\ln(dK'/dK)|_{K_c}}{\ln b} = 1.$$

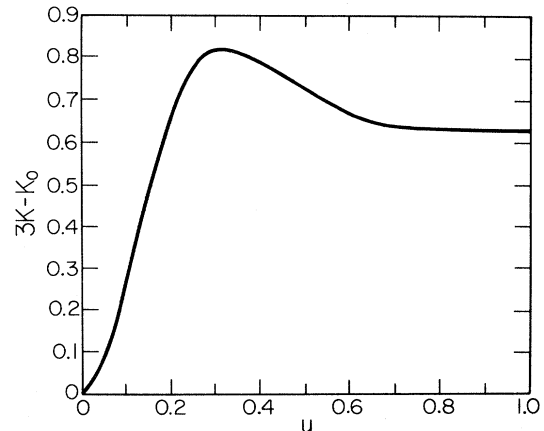


FIG. 3. Plot of  $3K - K_0$  vs  $u = \tanh K$ .

TABLE I. Comparison of renormalization-group (RG) with Monte Carlo (MC) and exact results for short-range two-spin-correlation functions at  $T = T_c$ .

	RG	MC and exact
$\epsilon(1,1)$	$\frac{10}{17} = 0.5882$	$0.5865 \pm 0.01^a$
$\epsilon(0,2)$	$\frac{490}{867} = 0.5652$	$0.5619^b$
$\epsilon(0,3)$	$\frac{150}{289} = 0.5190$	$0.5078^b$

<sup>a</sup>Monte Carlo results.

<sup>b</sup>Reference 19—results are exact to the four digits shown.

The only function I study below  $T_c$  is the magnetization. Above  $T_c$  the magnetization is zero; this fact is reproduced by the recursion relation, Eq. (3.4). The solution to Eq. (3.4) is plotted in Fig. 4. For comparison, the exact result<sup>11</sup> is

$$M = \left[ 1 - \frac{1}{16(1+u^3)u^3(1+u)^3} \right]^{1/8}. \quad (4.6)$$

The magnetization behaves as

$$M \sim D \left| \frac{u - u_c}{u_c} \right|^\beta \quad (4.7)$$

just below  $T_c$ . From Eq. (4.6) I obtain  $D=1.21$  and  $\beta=0.125$ , in comparison to the recursion solution to Eq. (3.4) which yields  $D=1.34$  and  $\beta=0.113$ . The agreement away from the critical point is much better. The inclusion of symmetry-breaking effects in  $T(\mu, \sigma)$  for  $T < T_c$  should improve the agreement near the critical point.<sup>7</sup>

The solution to the recursion relation for the specific heat, Eq. (3.15), is plotted in Fig. 5 and compared to the series results.<sup>12</sup> The exact result for the specific heat has a logarithmic singularity at  $T_c$ . The result for the specific

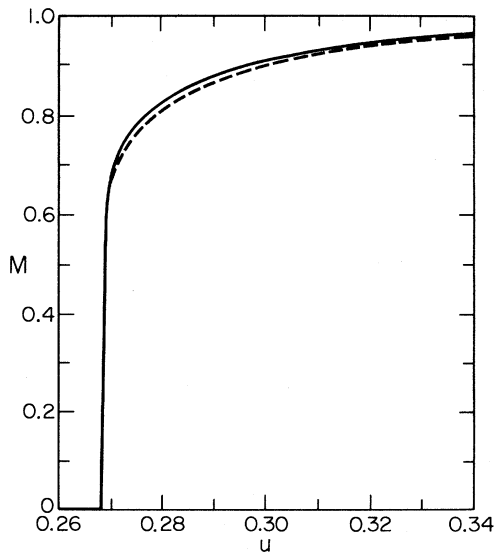


FIG. 4. Plot of the magnetization vs  $u = \tanh K$ . Solid line is the result of iterating Eq. (3.4) while the dashed line is the exact solution (Ref. 11).

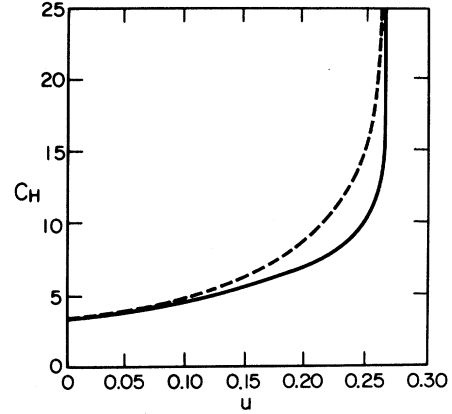


FIG. 5. Plot of the specific heat vs  $u = \tanh K$ . Solid line is the solution to Eq. (3.15) which diverges as  $|(u - u_c)/u_c|^{-0.068}$ . Dashed line is the series result (Ref. 12).

heat on the square lattice remains finite at  $T_c$ , giving  $\alpha=0$  for the critical exponent. On the triangular lattice, the renormalization group predicts a divergence for the specific heat with exponent  $\alpha = \ln \frac{300}{289} / \ln \sqrt{3} = 0.068$ . However, a change in the calculated value of the spin rescaling  $\nu_1$  at  $T_c$  of 0.92% would give a logarithmic singularity. Despite the fact that the renormalization-group result diverges faster than the exact result at  $T_c$ , it remains smaller than the exact result until it is very near  $T_c$ . The overall agreement in Fig. 5 is good for small  $u$  (large  $T$ ), but only fair near  $T_c$ .

I now study the behavior of the susceptibility  $\chi$  by iterating Eq. (3.9) and find that near  $T_c$ ,  $\chi \sim C_+ |(u - u_c)/u_c|^\gamma$  with  $\gamma=1.771$  and  $C_+=0.9552$ . High-temperature series results give  $C_+=0.92421$ , a difference of 3%, and the estimate of  $\gamma$  differs from the exact value of  $\frac{7}{4}$  by 1.2%. A plot of  $\chi$  is shown in Fig. 6 for small values of  $\chi$ ; the agreement for larger values of  $\chi$  is also reasonable due to the accurate values for the critical exponent and amplitude.

For  $q \neq 0$ , the agreement between  $C(q)$  found from Eq. (3.6) and the series results is not as good as for  $q=0$ . A

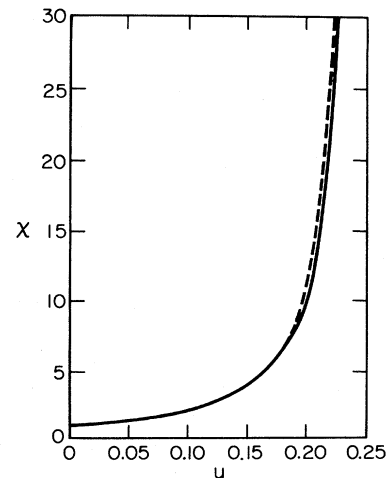


FIG. 6. Plot of the susceptibility  $\chi$  vs  $u = \tanh K$ . Solid line is the solution to Eq. (3.9) while the dashed line is the series result (Ref. 13).

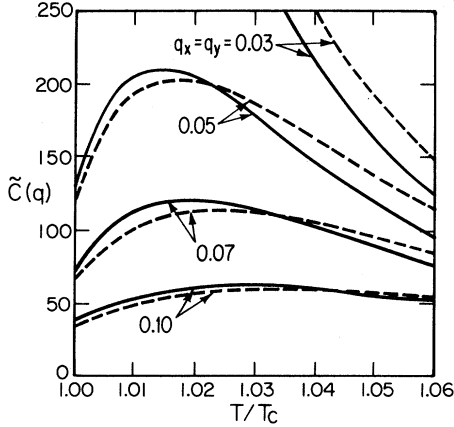


FIG. 7. Plot of  $C(q)$  against  $T$  for several fixed values of  $q_x = q_y$ . Solid lines are the result of iterating Eq. (3.6) while the dashed lines are the series result (Ref. 13).

plot of the results for  $C(q)$  versus  $\tanh K$  for various values of  $q$  is shown in Fig. 7. The curves compare well with the series results,<sup>13</sup> with the maximum difference typically less than 10%.

The values derived from the recursion relation for  $C(q)$  are generally the sum of positive and negative contributions, due to the possibility that  $f(q)$  in Eq. (3.7) can become negative. The equivalent function on the square lattice  $f_s = [1 - \cos(q_x)][1 - \cos(q_y)]$  is always positive. Thus, all of the terms obtained by iterating the analog of Eq. (3.6) are of the same sign; the relative error in the final answer is the same size as the relative error of the additive terms. For the triangular lattice, the relative error in the final answer can be much larger due to cancellation. For example, if I start the iteration near  $T_c$ , the negative contribution is generally about half the size of the final result for  $C(q)$ . Thus, significant cancellation must occur to achieve the agreement shown in Fig. 7.

In order to study the accuracy of the calculated  $C(q)$  at larger  $q$ , where  $f(q)$  is negative and the series are less reliable, I have performed Monte Carlo simulations of a lattice of 100 by 100 spins. I discarded the first 100 Monte Carlo steps for  $T$  away from  $T_c$  and the first 300 Monte Carlo steps for  $T$  near  $T_c$ . I sampled the system every 5 Monte Carlo steps and measured  $C(q)$ . For the large  $q$  that I used, widely separated parts of the lattice gave uncorrelated contributions to the average. I was able to obtain reasonable statistics after 7000 Monte Carlo steps. The renormalization-group solution is accurate to within 10% over the entire range of  $q$  and  $T$  studied; for example, at  $q_x = \pi/2$ ,  $q_y = 2\pi/\sqrt{3}$ , and  $u = 0.2$  I found  $C(q) = 0.437$  by the renormalization group and  $C(q) = 0.41 \pm 0.015$  in the simulations; at  $q_x = \pi$ ,  $q_y = 3.82$ , and  $u = 0.2$  I found 0.587 and  $0.56 \pm 0.02$ , respectively, for  $\tilde{C}(q)$ . Thus, I conclude that the oscillating sign of  $f(q)$  does not affect the accuracy of the static recursion relations.

## V. DYNAMICAL FORMALISM

To introduce dynamics, I study the Glauber model, in which the time evolution of a spin operator is given by

$$A(\sigma, t) = D_\sigma A(\sigma, t) = \sum_{\sigma'} D(\sigma, \sigma') A(\sigma', t), \quad (5.1)$$

where  $D(\sigma, \sigma')$  is the stochastic spin-flip operator, which can be written in the form

$$D(\sigma, \sigma') = -\frac{\alpha}{2} \sum_{i,a} \Lambda_{\sigma, \sigma'}^{[i,a]} \sigma'_{i,a} \sigma_{i,a} W_{i,a}(\sigma). \quad (5.2)$$

The constant  $\alpha$  determines the basic spin-flip rate,  $\Lambda_{\sigma, \sigma'}^{[i,a]}$  is a product of  $\delta$  functions

$$\Lambda_{\sigma, \sigma'}^{[i,a]} = \prod_{j,b (\neq i,a)} \delta_{\sigma_{j,b}, \sigma'_{j,b}},$$

which ensures that each term in  $D_\sigma$  changes, at most, one spin at a time and

$$E_{i,a} = K \sum_{\langle ia, jb \rangle} \sigma_{j,b}$$

(the sum is over the nearest neighbors of the site  $i,a$ ) is the energy associated with a spin flip at site  $i,a$ . The function  $W_{i,a}$  depends only on the spin  $\sigma_{i,a}$  and its six nearest neighbors.

The spin-flip operator  $D_\sigma$  must keep the equilibrium probability distribution constant in time. I only consider spin-flip operators that obey the stronger condition of detailed balance [which, with the form of  $D_\sigma$  in Eq. (5.2), implies the above condition on the probability distribution]

$$D(\sigma, \sigma') P(\sigma') = D(\sigma', \sigma) P(\sigma), \quad (5.3)$$

or equivalently,

$$\frac{W_{i,a}(\sigma) |_{\sigma_{i,a}=+1}}{W_{i,a}(\sigma) |_{\sigma_{i,a}=-1}} = e^{-2E_{i,a}(\sigma)}. \quad (5.4)$$

Note that with regard to  $E_{i,a}(\sigma)$ , all pairs of neighbors of the site  $i,a$  are equivalent. Thus I can restrict my attention to functions  $W_{i,a}$  that preserve the equivalence of each pair of neighbors. I write  $W_{i,a}$  in the form

$$W_{i,a}(\sigma) = 1 + a_1 \sigma^s + a_2 g_2(\sigma) + a_3 g_3(\sigma), \quad (5.5)$$

where the function  $\sigma^s$  is the sum of all neighbors of  $\sigma_{i,a}$ , the function  $g_2$  is a sum of all pairs of neighbors of  $\sigma_{i,a}$ , and the function  $g_3$  is a sum of all sets of three neighbors of  $\sigma_{i,a}$ . I find that the resulting spin-flip operator

$$D(\sigma, \sigma') = -\frac{\alpha}{2} \sum_{i,a} \Lambda_{\sigma, \sigma'}^{[i,a]} W_{i,a}(\sigma) \sigma_{i,a} \sigma'_{i,a}, \quad (5.6)$$

satisfies detailed balance and stationarity if  $a_i$  satisfies<sup>14</sup>

$$a_1 = -\frac{1}{2} \tanh(2K), \quad (5.7a)$$

$$a_2 = \frac{1}{5} \tanh^2(2K), \quad (5.7b)$$

and

$$a_3 = -\frac{1}{20} \tanh^3(2K). \quad (5.7c)$$

Then,  $D_\sigma$  is the generalization for the triangular lattice of the "minimal coupling operator" defined on the square lattice.<sup>5</sup>

In order to obtain dynamical recursion relations, I must derive a perturbation expansion of  $D_\sigma$  and require  $D_\sigma$  to

$$\overline{W'_{i,a} = 1 + b_1 \sigma_{i,a} \sigma_C^s + b_2 \sigma_{i,a} \sigma_I^c + c_1 \sigma_I^n + c_2 \sigma_I^s \sigma_C^s + c_3 \sigma_C^c + d_1 \sigma_{i,a} \sigma_I^T + d_2 \sigma_{i,a} \sigma_C^s \sigma_I^n + d_3 \sigma_{i,a} \sigma_C^s \sigma_I^s}, \quad (5.8a)$$

where

$$\sigma_C^s = \sigma_{i,a+1} + \sigma_{i,a-1}, \quad (5.8b)$$

$$\sigma_I^c = \sigma_{i-3\delta_{a+1},a+1} + \sigma_{i-3\delta_{a-1},a-1} + \sigma_{i+3\delta_{a+1},a+1} + \sigma_{i+3\delta_{a-1},a-1}, \quad (5.8c)$$

$$\begin{aligned} \sigma_I^n = & \sigma_{i-3\delta_{a+1},a+1} + \sigma_{i+3\delta_{a-1},a-1} + \sigma_{i-3\delta_{a+1},a+1} + \sigma_{i+3\delta_{a-1},a-1} + \sigma_{i-3\delta_{a+1},a+1} + \sigma_{i+3\delta_{a-1},a-1} \\ & + \sigma_{i-3\delta_{a-1},a-1} + \sigma_{i+3\delta_{a+1},a+1} + \sigma_{i-3\delta_{a-1},a-1} + \sigma_{i+3\delta_{a+1},a+1} + \sigma_{i+3\delta_{a-1},a-1} + \sigma_{i+3\delta_{a+1},a-1}, \end{aligned} \quad (5.8d)$$

$$\sigma_C^c = \sigma_{i,a+1} \sigma_{i,a-1}, \quad (5.8e)$$

and

$$\begin{aligned} \sigma_I^T = & \sigma_{i-3\delta_{a+1},a+1} + \sigma_{i-3\delta_{a-1},a-1} + \sigma_{i+3\delta_{a+1},a+1} + \sigma_{i-3\delta_{a+1},a+1} + \sigma_{i-3\delta_{a-1},a-1} + \sigma_{i+3\delta_{a-1},a-1} \\ & + \sigma_{i-3\delta_{a+1},a+1} + \sigma_{i+3\delta_{a-1},a-1} + \sigma_{i+3\delta_{a-1},a-1} + \sigma_{i-3\delta_{a-1},a-1} + \sigma_{i+3\delta_{a+1},a+1} + \sigma_{i+3\delta_{a-1},a-1}. \end{aligned} \quad (5.8f)$$

The generalization of the detailed balance condition, Eq. (5.4), is

$$\frac{W'_{i,a}(\sigma) |_{\sigma_{i,a}=+1}}{W'_{i,a}(\sigma) |_{\sigma_{i,a}=-1}} = e^{-2(K_c \sigma_C^s + K_I \sigma_I^c)}. \quad (5.9)$$

Equation (5.9) is equivalent to seven independent conditions involving the eight parameters  $b_i$ ,  $c_i$ , and  $d_i$ . An additional equation is needed to specify the expansion parameters and guarantee that Eq. (5.8a) reduces to (5.5) in the isotropic limit. Since I have already satisfied detailed balance and stationarity, I am free to choose the reasonable condition that  $c_3$  is at least second order in the intercellular coupling. This choice specifies the coefficients to first order and ensures that  $K'(K)$  derived by static and dynamical methods agrees to that order. I find that  $b_1$  contributes to lowest order, and  $b_2$  and  $c_2$  contribute at first order.  $W'$  becomes, to first order,

$$W'_{i,a} = 1 - \frac{1}{2} a_c \sigma_{i,a} \sigma_C^s - \frac{1}{2} a_I \sigma_{i,a} \sigma_I^c + \frac{1}{4} a_I a_c \sigma_C \sigma_I \quad (5.10a)$$

with

$$a_I = \tanh(2K_I) \quad (5.10b)$$

and

$$a_c = \tanh(2K_C). \quad (5.10c)$$

## VI. DYNAMICAL RECURSION RELATIONS AND RESULTS

Given the expansion for  $D_\sigma$ , the formalism for deriving dynamical recursion relations can be directly applied.<sup>4,5</sup> I have already ensured that the correlations are short range in space for  $T \neq T_c$ ; I must now ensure that the operators and correlations remain local in time as well. Most straightforward renormalization procedures lead to nonlocal, non-Markovian contributions to the renormalized

satisfy detailed balance and stationarity order by order in  $\lambda$ . To expand  $D_\sigma$  I rewrite Eq. (5.5) to distinguish between products of spins in the same cell and products of spins in different cells. Equation (5.5) then becomes

spin-flip operator  $D_\sigma$ . I avoid these problems by requiring that my coarse-graining operator  $T(\mu, \sigma)$  satisfy<sup>4,5</sup>

$$D_\sigma T(\mu, \sigma) = D_\mu T(\mu, \sigma). \quad (6.1)$$

In addition, this requirement ensures that  $D_\sigma$  satisfies stationarity and detailed balance on the renormalized lattice.<sup>5</sup>

To zeroth order, Eq. (6.1) is satisfied by my static transformation given by Eqs. (2.16) and (2.17) as long as  $\psi$  is any eigenfunction of the zeroth-order spin-flip operator. In addition to the expansion of  $W$  found in Sec. V, I also introduce an expansion of

$$\alpha(\lambda) = \alpha_0 + \sum_{n=1}^{\infty} \alpha_n \lambda^n.$$

Upon combining both expansions, I obtain the lowest-order spin-flip operator

$$D^0(\sigma, \sigma') = -\frac{\alpha_0}{2} \sum_{i,a} \Lambda_{\sigma, \sigma'}^{[i,a]} \sigma_{i,a} \sigma'_{i,a} W_{i,a}(\sigma) \quad (6.2a)$$

with

$$W_{i,a}^0 = 1 - \frac{a_c}{2} \sigma_{i,a} \sigma_C^s. \quad (6.2b)$$

The odd eigenfunctions and eigenvalues of  $D^0$  are given in Table II. The slowest odd mode is

$$\psi^{(1)}(\sigma) = n_1 \sum_a \sigma_{i,a}$$

with eigenvalue  $\lambda^{(1)} = \alpha_0(1 - a_0)$ . Thus, my previous static transformation maps  $\sigma_{i,a}$  onto the slowest mode of the renormalized cell. This property of leaving the slowest evolving mode in the problem while summing out the faster modes implies that the  $T(\mu, \sigma)$  chosen from static considerations is also appropriate for the dynamics. To lowest order, I find for the renormalized spin-flip operator



TABLE II. List of the odd eigenvalues of the zeroth-order spin-flip operator  $D_\sigma^0 \psi_i^{(n)} = -\lambda_i^{(n)} \psi_i^{(n)}$ . The  $\phi$ 's are defined as  $\phi_1(q) = \sum_a e^{iqa} \sigma_{i,a}$ ,  $\phi_3 = \prod_a \sigma_{i,a}$ .

$n$	$\lambda^{(n)}/\alpha_0$	$\psi^{(n)}$	$N_n$
1	$1 - a_0$	$\frac{1}{N_1} \phi_1(0)$	$\left[ 3 \left( \frac{2+a_0}{2-a_0} \right) \right]^{1/2}$
2	$1 + a_0/2$	$\frac{1}{N_2} \phi_1 \left( \frac{2\pi}{3} \right)$	$\left[ 6 \left( \frac{1-a_0}{2-a_0} \right) \right]^{1/2}$
3	$1 + a_0/2$	$\frac{1}{N_2} \phi_1 \left( \frac{4\pi}{3} \right)$	
4	3	$\frac{1}{N_4} \left[ \phi_3 - \frac{a_0}{2+a_0} \phi_1(0) \right]$	$2 \left( \frac{1-a_0^2}{4-a_0^2} \right)^{1/2}$

$$D^0(\mu, \mu') = -\frac{\lambda'}{2} \sum_i \Lambda_{\mu, \mu'}^{[i]} \mu_i \mu'_i. \quad (6.3)$$

I find that to lowest order

$$\alpha' = \lambda^{(1)}. \quad (6.4)$$

To find the first-order contribution to the spin-flip operator, I expand Eq. (6.1) order by order and use Eq. (2.12) to obtain

$$D^1(\sigma, \sigma') P_0(\sigma') = \left\langle \sum_{\sigma'} T_0(\mu, \sigma) D^1(\sigma, \sigma') T_0(\mu, \sigma') \right\rangle_0, \quad (6.5)$$

with

$$D^1(\sigma, \sigma') = -\frac{\alpha_0}{2} \sum_{i,a} W_{i,a}(\sigma) \Lambda_{\sigma, \sigma'}^{[i,a]} \sigma_{i,a} \sigma'_{i,a}, \quad (6.6)$$

and where  $W_{i,a}$  is the first-order part of Eq. (5.10). The averages over the uncoupled probability distribution can be evaluated to give

$$D^{(1)}(\sigma, \sigma') = -\frac{\alpha_0}{3} a_I (1 - r a_C) \sum_{i,a} \Lambda_{\mu, \mu'}^{[i]} \mu_i \mu'_i + \delta'_a, \quad (6.7)$$

where  $r$  is defined in Eq. (2.6) and  $\delta'_a = 3\delta_a$ . There is also a contribution to  $D^{(1)}$  which involves  $\alpha_1$  times  $W^{(0)}$ ; this term can be grouped with  $D^{(0)}$ , leading to a replacement of  $\alpha_0$  by  $\alpha_0 + \lambda \alpha_1$  in the formula for  $D^{(1)}$ . With the use of the fact that  $(1 - r a_C) = 3\lambda^{(1)} v_1^2$  and that  $\mu_i^2 = 1$ , I collect the zeroth- and first-order terms to find

$$D(\mu, \mu') = -\frac{\alpha'}{2} \sum_i \Lambda_{\mu, \mu'}^{[i]} (1 - 2u_I v_1^2 \mu_i \mu'_i + \delta'_a). \quad (6.8)$$

The form of the spin-flip operator is preserved to first order, which is seen by comparing Eqs. (5.6) and (6.8). The recursion relation obtained by equating coefficients,  $u'_I = 2v_1^2 u_I$ , is consistent with Eq. (2.22) to first order. The rotation taking  $\bar{T}$  to  $T$  has no effect on  $D(\mu, \mu')$  obtained above and hence  $\bar{D} = D$  to first order.

I now consider recursion relations for the dynamical correlation function

$$C_{ia,jb}(t) = \langle \sigma_{i,a} e^{D_\sigma^0 t} \sigma_{j,b} \rangle. \quad (6.9)$$

I expand  $\sigma_{i,a}$  in terms of the complete set  $\{\psi^{(n)}\}$  of eigenfunctions of  $D^0$  and again use the projection operators to derive

$$C_{ia,jb}(t) = v_1^2 C'_{i,j}(t') + \delta_{i,j} \sum_{n=2}^4 v_n(a) v_n(b) e^{-\lambda^{(n)} t}, \quad (6.10)$$

where the sum runs over all odd eigenfunctions of  $D^0$  except for the slowest,  $v_n(a) = \langle \psi^{(n)} \sigma_{i,a} \rangle_0$ , and  $t' = \Delta t$  where  $\Delta = \alpha'/\alpha$  is the time-rescaling factor. Note that since  $\lambda^{(n)} > \lambda^{(1)}$  for  $n > 1$ , the inhomogeneous term in Eq. (6.10) decays faster than the  $C'(t')$  term. The sum in Eq. (6.10) would include the even eigenfunctions of  $D^0$  as well, but the  $v_n(a)$  are zero for those modes.

The Fourier transform of Eq. (6.10) yields the following recursion relation for  $C(q, \omega)$ :

$$C(q, \omega) = \frac{v_1^2 f(q)}{\Delta} C'(q', \omega') + 2 \sum_{n=2}^4 \frac{f_n(q) \lambda^{(n)}}{\omega^2 + \lambda^{(n)2}}, \quad (6.11a)$$

where

$$f_n(q) = \frac{1}{3} \sum_a v_n^*(a) v_n(a) + v_n^*(a) v_n(a+1) + v_n^*(a+1) v_n(a), \quad (6.11b)$$

$\omega' = \omega/\Delta$ , and  $q'$  was defined in Eqs. (3.8).

As in the static case, the inhomogeneous term in Eq. (6.11a) vanishes in the limit  $q \rightarrow 0$ . In the limits  $q \rightarrow 0$  and  $\omega \rightarrow 0$ , I obtain

$$C(0,0) = \frac{3v_1^2}{\Delta} C'(0,0). \quad (6.12)$$

I can use Eq. (6.12) to determine the expansion parameter  $\alpha_0$ . I note that  $\alpha_0$  is related to  $\Delta$  by Eq. (6.4) and the formula for  $\lambda^{(1)}$ :

$$\Delta = \frac{\alpha_0}{\alpha} (1 - a_0). \quad (6.13)$$

I follow Mazenko and Valls and determine  $\Delta$  by relating  $C(0,0)$  to memory functions; these in turn are related to  $\langle W_{i,a} \rangle$ .<sup>4,5</sup> One finds that  $\Delta$  is the ratio of characteristic frequencies:<sup>4,5</sup>

$$\Delta = \frac{\chi' \langle W_{i,a} \rangle}{\chi \langle W_{i,a} \rangle'} \quad (6.14)$$

Included in  $\langle W_{i,a} \rangle$  are two-spin correlations  $\epsilon(1,1)$  and four-spin correlations whose temperature dependence is not known in closed form. To find these functions I calculate them using the static renormalization group. I define the functions

$$S_1 = \langle \sigma_{i,a} \sigma_{i,a+1} \sigma_{i,a-1} \sigma_{i+3\delta_{a,a-1}} \rangle, \quad (6.15a)$$

$$S_2 = \langle \sigma_{i,a} \sigma_{i,a+1} \sigma_{i,a-1} \sigma_{i-3\delta_{a+1,a+1}} \rangle, \quad (6.15b)$$

$$S_3 = \langle \sigma_{i,a} \sigma_{i,a+1} \sigma_{i+3\delta_{a,a+1}} \sigma_{i-3\delta_{a+1,a+1}} \rangle. \quad (6.15c)$$

Before the renormalization group is applied to these functions, a further average over all translationally and rotationally equivalent spin configurations should be performed. I find that

$$\begin{aligned} \langle W_{i,a} \rangle = & 1 + 6a_1 \epsilon(0,1) \\ & + 12a_2 [2\epsilon(0,1) + 2\epsilon(1,1) + \epsilon(0,2)] \\ & + 16a_3 (6S_1 + S_2 + 3S_3), \end{aligned} \quad (6.16)$$

where  $a_1$ ,  $a_2$ , and  $a_3$  are defined in Eqs. (5.7). The recursion relations for the functions in Eqs. (6.15) can be found as usual by the methods of Sec. III:

$$S_1 = \frac{1}{6} [v_1^4 s_2' + r(1 + 2v_1^2) \epsilon'(0,1) + v_1^2 r \epsilon'(1,1) + r^2], \quad (6.17a)$$

$$S_2 = \frac{1}{3} r (1 + 2v_1^2) \epsilon'(0,1), \quad (6.17b)$$

$$S_3 = r v_1^2 \epsilon'(0,1). \quad (6.17c)$$

The functions  $\epsilon(0,1)$  and  $\epsilon(0,2)$  can be computed exactly;  $\epsilon(1,1)$  is obtained from Eq. (3.13c).

I now evaluate the dynamic recursion relations numerically. I first examine the accuracy of the approximation for  $\Lambda$  obtained by substituting the solution of Eqs. (6.17) into Eq. (6.16). Since there are no exact results published for the four-spin correlations, I used Monte Carlo simulations to find their values. I was able to obtain a good accuracy for the local-spin correlations with only 500 Monte Carlo steps since I performed both a space and time average. Both the Monte Carlo and renormalization-group results for the functions  $S_3$  and  $S_1$  are plotted in Fig. 8; the difference between the results for the two methods is generally less than 10%. Since the largest errors occur where the correlations are small, I expect that my calculation differs from the exact result for  $\langle W_{i,a} \rangle$  by less than 10%. The result for  $\Delta$  is plotted in Fig. 9.

Next, I iterate Eq. (6.10) to find the autocorrelation function  $C_{ia,ia}(t)$ . In the infinite- $T$  limit, the spins are uncorrelated and

$$C_{ia,ia}(t) |_{u=0} = e^{-\alpha t}, \quad (6.18)$$

which is plotted as the dotted line in Fig. 10. At lower  $T$ , the correlations decay more slowly, until at  $T_c$  a long-time tail should appear. Our results for  $u=0.01$  decay slightly faster than those given by Eq. (6.18), but they overshoot by no more than 3%. As  $T$  is lowered the

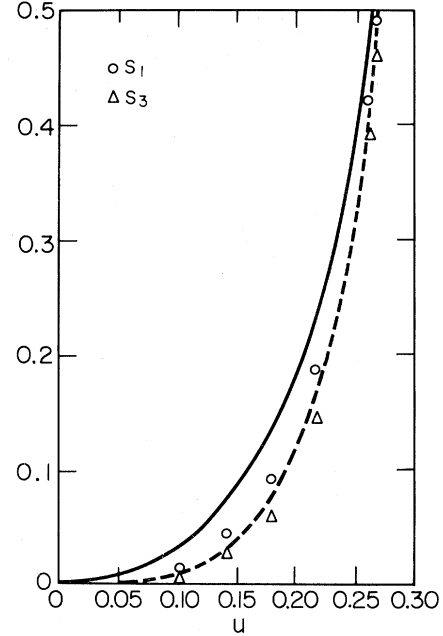


FIG. 8. Comparison of the values for the four-spin-correlation functions found by renormalization-group and Monte Carlo simulation. Dashed line is the result of iterating Eq. (6.17c) for  $S_3$  while the triangles are the Monte Carlo results for that function. Solid line is the solution to Eq. (6.17a) for  $S_1$  and the circles are the corresponding Monte Carlo results. The size of the symbols is the size of the estimated error in the Monte Carlo data.

correlation function does begin to decay very slowly, as shown in Fig. 10.

I now iterate Eqs. (6.11) to find  $C(q,\omega)$ . The results are plotted in Fig. 11, for fixed  $q$ . There is no calculation, known to the author, of the dynamic structure factor for the Ising model on the triangular lattice. The results are reasonable for small  $\omega$ ; for larger  $\omega$  and  $T$  near  $T_c$ , note that  $C(q,\omega)$  is not a monotonic function of  $T$ . For example, as  $u$  increases from  $u=0.25$  to  $u=u_c \cong 0.2679$  ( $T$  decreases),  $C(q,\omega)$  initially decreases 30–50% before rising sharply. As  $T_c$  is approached, this nonmonotonic behavior occurs for smaller  $\omega$ .

These nonmonotonic results are probably due to the sensitivity of Eqs. (6.11) to slight numerical errors rather

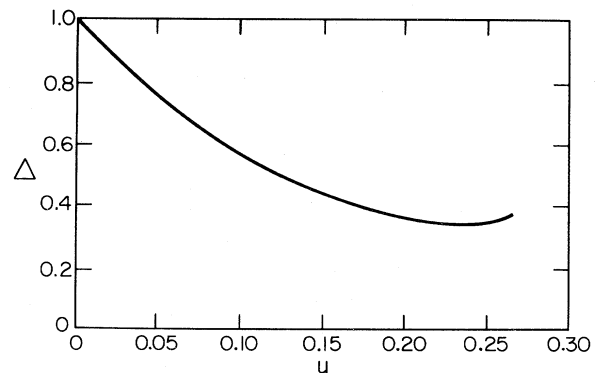


FIG. 9. Plot of the time-rescaling factor  $\Delta$  vs  $u = \tanh K$  for  $T > T_c$ .

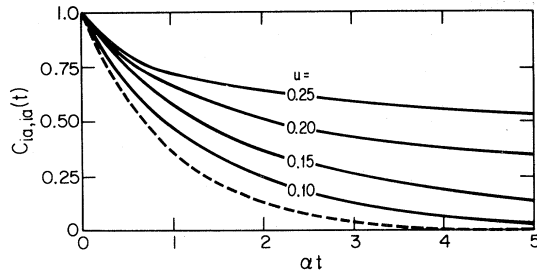


FIG. 10. Plot of the spin autocorrelation function,  $C_{ia,ia}(t)$ , as a function of time;  $\alpha$  is a microscopic inverse time scale. Dotted line is the exact infinite  $T(u=0)$  result.

than a fundamental flaw in the method. Near  $T_c$  it is necessary to iterate many times to reach sufficiently large  $T$ , such that  $C(q, \omega)$  can be calculated. Upon each iteration, a factor of  $1/\Delta$  in Eq. (6.11a) increases the importance of any numerical inaccuracy. For a value of  $T$  where the nonmonotonicity occurs, typically ten iterations are required. An indication of the sensitivity of Eqs. (6.11) to small numerical errors is that the difference between using single and double precision on an IBM model no. 3081 computer to evaluate the iteration can be over 10%. This sensitivity is due to the fact that  $f(q)$  can change sign and that the structure factor is the sum of positive and negative contributions. Although single precision is sufficient to calculate the cancellation for the statics, greater precision is required for the dynamics. The results for  $C(q, \omega)$  did not change further when quadruple precision was used. Hence, numerical precision is not the cause of the nonmonotonicity but indicates that Eqs. (6.11) are very sensitive to small errors.

One possible error is in the calculation of  $\Delta$ . One way

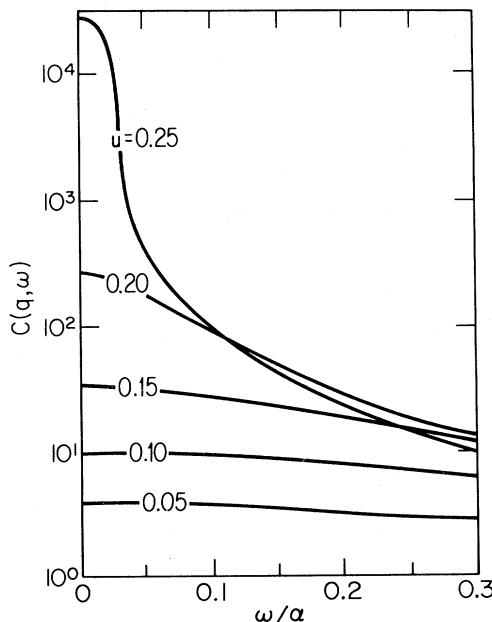


FIG. 11. Plot of the renormalization-group result for the dynamic structure factor versus frequency for a fixed value of the wave vector. Behavior for larger  $\omega$  and  $u$  is anomalous; the correlations should increase monotonically with  $u$ .

of improving the accuracy is to compute the four-spin-correlation functions using a first-order renormalization-group calculation. Also, one could take the entire dynamical calculation to one higher order. It was found in the square lattice calculation that many qualitative deficiencies in the results below  $T_c$  (infinite susceptibility and negative correlation length) could be eliminated by taking one more order in the perturbation expansion<sup>15</sup> as well as by introducing broken-symmetry effects.<sup>7</sup>

## VII. DISCUSSION

I have found that the renormalization-group method of Mazenko and Valls<sup>5</sup> can be extended to the triangular lattice to give good results for the static properties. The method yields accurate results for the universal quantities, such as critical exponents, and also for nonuniversal (lattice-dependent) quantities, such as amplitudes, on both the square and triangular lattices. All functions that are averages of spins can be calculated for all temperatures as a function of distance or wavelength. While the recursion relations derived here can be used for  $T < T_c$ , the inclusion of symmetry-breaking (magnetic field) effects would increase their accuracy. For correlation functions of a moderate number of spin variables, from which all thermodynamic functions of interest can be obtained, the lowest-order recursion relations generated by the methods used here can be derived easily and provide a relatively accurate value of the function for general temperature and wavelength.

The results for the dynamics are less clear. The calculated autocorrelation function exhibits the correct qualitative behavior, and agrees with the known high-temperature behavior. There are no results known to the author for the dynamic structure factor  $C(q, \omega)$  for general  $(q, \omega)$ , and  $T$  to make quantitative comparisons. The nonmonotonicity in  $C(q, \omega)$  is qualitatively incorrect, but it is expected that with a more accurate determination of the expansion parameters the method will give qualitatively correct results for the dynamical quantities for all parameter values.

Since our real-space renormalization-group method accurately predicts lattice-dependent quantities, it should be a valuable tool to study frustration, which is a lattice-dependent phenomenon. For antiferromagnetic coupling on the square lattice, flipping the sign of alternate spins maps the problem onto a ferromagnetic coupling of the same strength; our method predicts this well-known mapping.<sup>10</sup> On the triangular lattice, however, there is no such mapping, since each elementary triangular plaquette is "frustrated" by antiferromagnetic couplings and the ground state is infinitely degenerate. The application of the methods used here to the antiferromagnetic Ising model on the triangular lattice should yield important insights into the dynamics of frustration in such models.

## ACKNOWLEDGMENTS

I would like to thank Gene Mazenko and Oriol Valls for many useful discussions, and Harvey Gould for con-

versations and extensive comments on the paper. I would also like to thank Scott Bradlow for assistance with the spin-flip operator expansions, Dieter Heermann for help on the Monte Carlo simulations, and Sid Redner for help with the series expansions. I gratefully acknowledge sup-

port from National Science Foundation and a Sigma Xi Research Grant. The Center for Polymer Studies (Boston University) is partially supported by grants from the National Science Foundation, U.S. Army Research Office, and the U.S. Office of Naval Research.

\*Present and permanent address.

<sup>1</sup>T. Niemeijer and J. M. J. van Leeuwen, in *Phase Transitions and Critical Phenomena*, edited by C. Domb and M. S. Green (Academic, New York, 1976), Vol. 6; and in *Real Space Renormalization Group*, edited by T. W. Burkhardt and J. M. J. van Leeuwen (Springer, New York, 1982).

<sup>2</sup>M. Nauenberg and B. Nienhuis, *Phys. Rev. Lett.* **33**, 1598 (1974).

<sup>3</sup>Y. Achiam and J. Kosterlitz, *Phys. Rev. Lett.* **41**, 128 (1978); Y. Achiam, *J. Phys. A* **13**, 1355 (1980); W. Kinzel, *Z. Phys. B* **29**, 361 (1978); U. Dekker and F. Haake, *ibid.* **36**, 379 (1980); S. Ma, *Phys. Rev. B* **19**, 4824 (1979); J. O. Indeku, A. L. Stella, and L. Zhang, report (unpublished).

<sup>4</sup>G. F. Mazenko, M. J. Nolan, and O. T. Valls, *Phys. Rev. Lett.* **41**, 500 (1978); *Phys. Rev. B* **22**, 1263 (1980); **22**, 1275 (1980), and references therein.

<sup>5</sup>G. F. Mazenko and O. T. Valls, *Phys. Rev. B* **24**, 1404 (1981); and in *Real Space Renormalization Group*, edited by T. W. Burkhardt and J. M. J. van Leeuwen (Springer, New York,

1982).

<sup>6</sup>R. Swendsen, in *Real Space Renormalization Group*, edited by T. W. Burkhardt and J. M. J. van Leeuwen (Springer, New York, 1982).

<sup>7</sup>G. F. Mazenko and O. T. Valls, *Phys. Rev. B* **24**, 1419 (1981).

<sup>8</sup>G. Mazenko and O. T. Valls, *Phys. Rev. B* **27**, 6811 (1983).

<sup>9</sup>In the antiferromagnetic case, there is no such requirement, and one expects  $\psi$  to be related to a "staggered" magnetization. The functions  $\psi_{\pm} = \sum_a \sigma_{i,a} e^{\pm i(2\pi/3)qa}$  are a more appropriate choice; these are the slowest modes of the cell to lowest order in  $\lambda$ .

<sup>10</sup>L. P. Kadanoff, *Ann. Phys. (N.Y.)* **100**, 359 (1976).

<sup>11</sup>J. Stephenson, *J. Math. Phys.* **5**, 1009 (1964).

<sup>12</sup>C. Domb, in *Phase Transitions and Critical Phenomena*, edited by C. Domb and M. S. Green (Academic, New York, 1974), Vol. 3.

<sup>13</sup>M. E. Fisher and R. J. Burford, *Phys. Rev.* **156**, 583 (1967).

<sup>14</sup>S. Bradlow (unpublished).

<sup>15</sup>G. F. Mazenko (private communication).